

# Effects of Bulk Colloidal Stability on Adsorption Layers of Poly(diallyldimethylammonium Chloride)/Sodium Dodecyl Sulfate at the Air–Water Interface Studied by Neutron Reflectometry

Richard A. Campbell,<sup>\*,†</sup> Marianna Yanez Arteta,<sup>‡</sup> Anna Angus-Smyth,<sup>†,§</sup> Tommy Nylander,<sup>‡</sup> and Imre Varga<sup>\*,||</sup>

<sup>†</sup>Institut Laue-Langevin, 6 rue Jules Horowitz, BP 156, 38042 Grenoble Cedex 9, France

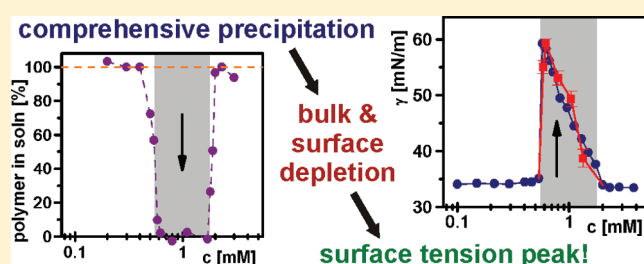
<sup>‡</sup>Department of Physical Chemistry, Lund University, P.O. Box 124, S-221 00 Lund, Sweden

<sup>§</sup>Department of Chemistry, Durham University, South Road, DH1 3LE, United Kingdom

<sup>||</sup>Institute of Chemistry, Eötvös Loránd University, Budapest 112, P.O. Box 32, H-1518 Hungary

## S Supporting Information

**ABSTRACT:** We show for the oppositely charged system poly(diallyldimethylammonium chloride)/sodium dodecyl sulfate that the cliff edge peak in its surface tension isotherm results from the comprehensive precipitation of bulk complexes into sediment, leaving a supernatant that is virtually transparent and a depleted adsorption layer at the air/water interface. The aggregation and settling processes take about 3 days to reach completion and occur at bulk compositions around charge neutrality of the complexes which lack long-term colloidal stability. We demonstrate excellent quantitative agreement between the measured surface tension values and a peak calculated from the surface excess of surfactant in the precipitation region measured by neutron reflectometry, using the approximation that there is no polymer left in the liquid phase. The nonequilibrium nature of the system is emphasized by the production of very different interfacial properties from equivalent aged samples that are handled differently. We go on to outline our perspective on the “true equilibrium” state of this intriguing system and conclude with a comment on its practical relevance given that the interfacial properties can be so readily influenced by the handling of kinetically trapped bulk aggregates.



## INTRODUCTION

Oppositely charged polyelectrolyte/surfactant (P/S) mixtures are essential components of countless products such as detergents, paints, shampoos, and conditioners and are also used in the food industry.<sup>1–3</sup> Also, the strong attractive interactions of surfactants with charged biological macromolecules such as proteins or DNA play an important role in biological processes<sup>4</sup> as well as in medical applications such as drug delivery.<sup>5,6</sup> It is important to understand the interactions of such species both in the bulk and at surfaces to predict their physicochemical behavior and in cases optimize performance.

The strong bulk association of oppositely charged P/S mixtures gives rise to rich phase behavior,<sup>2,7,8</sup> which has attracted considerable interest in the last two decades. At low bulk surfactant concentrations the mixtures are transparent. As the surfactant concentration increases, the net charge of the P/S complexes decreases until they lose their colloidal stability, and associative phase separation occurs which makes the solution turbid; i.e., a concentrated phase enriched in both polymer and surfactant separates from a dilute aqueous phase containing mostly small ions.<sup>9,10</sup> On the basis of the classical model of cooperative surfactant binding,<sup>3,11,12</sup> this phase behavior is

usually interpreted in terms of the formation of micelle-like surfactant aggregates along the polyelectrolyte chains, which starts at the critical aggregation concentration. At even higher ratios, charge reversal of the P/S complexes takes place due to the binding of surfactant aggregates, and solutions may become transparent again.<sup>9,11,13</sup>

In recent years, the importance of nonequilibrium states in oppositely charged P/S systems has become increasingly acknowledged. Several studies including those of Naderi et al.<sup>14,15</sup> and Mészáros et al.<sup>16</sup> have demonstrated that the mixing protocol used affects the formation of kinetically trapped nonequilibrium aggregates in a range of P/S systems. As a consequence, a mechanism based on the adsorption of surfactant molecules to the surface of collapsed particles leading to the formation of an electrostatically stabilized dispersion has been proposed in the high surfactant concentration range.<sup>16–19</sup>

At the solid/liquid interface, it is well-established that P/S systems undergo a strong attractive interaction (e.g.,

**Received:** September 14, 2011

**Revised:** November 12, 2011

**Published:** November 15, 2011

polyelectrolytes on oppositely charged surfaces) to form kinetically arrested states.<sup>20</sup> To obtain reproducible experimental results, the practical methodologies have to be strictly controlled. The order of changes to the system including addition of electrolyte and polyelectrolyte,<sup>21–23</sup> changing pH values,<sup>24,25</sup> and addition of polyelectrolyte and oppositely charged surfactant<sup>26–30</sup> has a profound effect on the structure and composition of the adsorbed material. Furthermore, it has been shown that such systems can adopt interfacial structures that do not reach equilibrium on experimentally accessible time scales.<sup>31,32</sup> This body of work has important repercussions for potential applications.

At the air/water interface, studies of a range of oppositely charged P/S systems have shown that at low bulk surfactant concentrations the presence of polyelectrolyte lowers the surface tension values significantly.<sup>33–38</sup> Thomas, Penfold, and co-workers principally used neutron reflectometry (NR)<sup>39</sup> to deliver an extensive characterization of the steady-state structure and composition of adsorption layers at the air/liquid interface.<sup>40</sup> They have shown that P/S mixtures can self-assemble into a range of interfacial morphologies including monolayers,<sup>41</sup> trilayers,<sup>42</sup> pentalayers,<sup>43</sup> and multilayers.<sup>44</sup> Furthermore, they have classified systems into two broadly different types where “type 1” adsorbs strongly in the form of complexes and creates thick layers of several nanometers or more and “type 2” forms more compact layers and tends to exhibit a sharp peak in the surface tension isotherm.<sup>40</sup> Studies by Bergeron et al.<sup>36</sup> and Monteaux et al.<sup>37,38</sup> have shown that outside the precipitation region such mixtures can form surface gel layers at the air/water interface with surface aggregation taking place at much higher surfactant concentrations than bulk aggregation. Furthermore, in dynamic studies Noskov et al. attributed a decrease in surface elasticity near charge equivalence (i.e., stoichiometric mixing where the number of moles of polyelectrolyte charges in the system equals that of oppositely charged surfactant ions) to the formation of a heterogeneous film containing microgel particles.<sup>45–47</sup>

Despite such a range of studies of either the nonequilibrium nature of the bulk phase behavior or the interfacial properties, there have been relatively few studies that have set out to relate the two. One study which examined this link was that of Lourette et al. who showed that lysozyme/sodium dodecyl sulfate (SDS) mixtures are strongly influenced by kinetically trapped states that are highly pathway dependent.<sup>48</sup> Another study by Mezei et al. showed that the chosen solution preparation method has a major impact on surface tension isotherms for poly(vinyl amine)/SDS mixtures.<sup>18</sup> Also, Tonigold et al. showed that for poly(ethylene imine)/SDS mixtures at pH 4 kinetically trapped bulk particles were present at static air/water interfaces in amounts that could be related to the sample history.<sup>49</sup>

The focus of the present study is to establish a quantitative link between the composition of a strongly interacting P/S system at the air/water interface and nonequilibrium features in the bulk. The system we have chosen for this work is the oppositely charged mixture poly(diallyldimethylammonium chloride)/SDS (Pdadmac/SDS), of which the phase behavior has been extensively studied already. Dautzenberg showed that the pure polymer molecules have a radius of gyration of 22 nm, while surface-active P/S complexes increase in size from ~15 nm up to ~100 nm at compositions close to charge equivalence.<sup>50</sup> The molecular interactions in these complexes have been shown to be both hydrophobic and electrostatic in nature and are enhanced in

the presence of added inert electrolyte.<sup>51</sup> In the stoichiometric mixing range, the complexes have an ordered hexagonal internal structure,<sup>52</sup> while at higher surfactant concentrations transparent Pdadmac/SDS solutions are observed, containing an electrostatically stabilized dispersion of particles.<sup>53</sup>

In the original work on this system at the air/water interface using NR in 2002, Staples et al. identified a cliff edge peak in the surface tension;<sup>41</sup> i.e., as the bulk surfactant concentration is increased in solutions of constant polymer concentration there is a dramatic rise in the surface tension close to the point of charge equivalence. They noted that the bulk composition of the peak maximum coincides with bulk phase separation but stated that this could not explain the feature and instead attributed it to the onset of formation of nonsurface-active bulk complexes in favor of surface-active complexes.<sup>54</sup> On the basis of this hypothesis, a thermodynamic model to explain the surface tension data was formulated by Bell et al.<sup>55,56</sup> and applied to data from a variety of P/S systems by Penfold et al.<sup>57</sup> on the basis of a two-phase air/liquid equilibrium. In examining the adsorption at short time scales on an overflowing cylinder, Campbell et al. showed total depletion of polymer at the interface close to the point of charge equivalence, which led to the suggestion that compared with Bell’s model there is an additional species present in the system, namely, macroscopic polymer/surfactant aggregates.<sup>58</sup> Furthermore, Noskov et al. observed that in the absence of added inert electrolyte the surface tension peak is a transient phenomenon and that in the precipitation region there are microparticles embedded in the adsorption layers.<sup>45</sup> It may also be noted that cliff edge peaks or more gentle rises in surface tension isotherms can be found in a range of studies on oppositely charged synthetic P/S systems<sup>14,59–64</sup> and homopolypeptide/surfactant,<sup>65</sup> protein/surfactant,<sup>66</sup> and DNA/surfactant<sup>67</sup> mixtures.

Intrigued by the above studies that suggest that bulk aggregate formation may in fact have a considerable effect on the interfacial properties of the Pdadmac/SDS system, we set out to determine whether nonequilibrium effects in the bulk are in fact linked to the production of the cliff edge peak. Recently, we published a letter stating our new perspective on the cliff edge peak in the surface tension for this system.<sup>68</sup> We demonstrated that the peak occurs: (1) only after depletion of most of the surface-active material from solution due to a slow sedimentation process in the precipitation region and (2) only if mechanical stress to the sediment that can redisperse surface-active components is absolutely avoided. We also outlined the time scale of the appearance of the peak and demonstrated the nonequilibrium nature of the system by eliminating the peak for equivalent aged samples by changing the sample handling.

Although our letter demonstrated the link between the bulk phase behavior and the surface tension of the Pdadmac/SDS system, it did not connect these properties to the amount and composition of the material at the interface. As there is no accessible direct relation between the surface tension and surface excess of a strongly associating multicomponent system, the present study is devoted to the necessary quantification of the interfacial composition in the context of nonequilibrium aspects of the system. We describe a characterization of the Pdadmac/SDS system at the air/water interface using NR with the primary aim of understanding how the amounts of adsorbed polyelectrolyte and surfactant change across the precipitation region for three well-defined physical states of the system. The three states represent varying levels of equilibration, but none of them have actually reached chemical equilibrium, which we demonstrate is

inaccessible on practical time scales. Two questions are addressed in a discussion of the results. First, can precipitation of polymer and surfactant from the liquid phase result in sufficient depletion of interfacial material to cause directly the cliff edge peak? Second, what is the “true equilibrium” of this inherently nonequilibrium system? We conclude with a comment on the relevance of the cliff edge peak in terms of practical applications of such systems.

## EXPERIMENTAL SECTION

**Materials.** Deionized water was passed through a purification system (Milli-Q; total organic content = 4 ppb; resistivity = 18 m $\Omega$ ·cm). Pdadmac (100k–200k g/mol; Aldrich) was purified by dialysis (regenerated cellulose, 12k–14k molecular weight cutoff, Medicell International Ltd.) in pure water to give a stock solution of  $\sim 20\,000$  ppm free of low molecular weight impurities. The concentration of the polymer stock solution was determined by gravimetric analysis. Hydrogenous SDS (hSDS; Sigma, 99.9%) was recrystallized twice in ethanol, and each time the solutions were cooled over several hours to maximize the purity of the surfactant. The high purity of the surfactant was verified with surface tension measurements. Deuterated SDS (dSDS; Cambridge Isotopes, 99%) was used as received after checking for contamination with NMR and verifying the purity using surface tension and NR measurements. To be able to compare literature data for similar systems the present study was carried out with solutions at an ionic strength of 0.1 M using added NaCl (Merck; 99.99%).

**Sample Preparation.** The solutions made comprised 100 ppm Pdadmac at various SDS concentrations in 0.1 M NaCl at 25 °C. A standard mixing<sup>49</sup> approach was used to ensure that the polymer/surfactant mixing protocols were carried out under reasonably well-defined conditions.<sup>17</sup> This approach was used to minimize the formation of kinetically trapped, nonequilibrium aggregates as a result of concentration gradients present during mixing. The Pdadmac stock solution obtained after the dialysis process was diluted to 200 ppm in 0.1 M NaCl, and a stock solution of SDS ( $\sim 20$  mM) in 0.1 M NaCl was made fresh daily. To mix each solution, equal volumes (25–150 mL) of each of the Pdadmac/NaCl and SDS/NaCl solutions were poured together simultaneously. The mixed solution was then swirled gently for 3 s to mix the contents, of which either 35 mL was transferred by a glass pipet into the measurement vessel (fresh samples) or the entire solution was poured into a 100 mL volumetric flask for storage (aged samples). A 50 mL glass pipet was also used to transfer aged solutions to the measurement vessel to minimize the transfer of surface-trapped precipitate.<sup>49</sup> Immediately prior to measurement, the surface of each solution was aspirated for 5 s using a clean pipet attached to a water suction pump. This process served to remove any surface-trapped precipitate and allowed measurements of material adsorbed to a fresh surface. We have carried out several checks to confirm that this surface cleaning procedure does not result in measurable depletion of surface-active material from the bulk by comparing surface tension and ellipsometry data of samples that were aspirated lightly like those in the present work (30% loss of volume) with those aspirated heavily (90% volume loss) to observe smaller deviations of the measured values than the experimental error of the measurements.

**Surface Tension Measurements.** The surface tension measurements presented in Figures 2B, 4B, and 7B were recorded on

an automated Krüss ‘K10’ surface tension balance. A sand-blasted platinum Wilhelmy plate of width 20 mm, height 10 mm, and thickness 0.10 mm was immersed into liquid contained in a Petri dish, and then the plate was withdrawn until the bottom of the plate was parallel with the free liquid surface. The overall force  $F$  that acts on the plate was used to calculate the surface tension  $\gamma = F/2p_p \cos \theta$ , where  $p_p$  is the perimeter of the plate and  $\theta$  is the contact angle between the liquid and plate. The full wetting criterion  $\cos \theta = 1$  was assumed, supported by the use of a sand-blasted plate<sup>69</sup> and no notable discrepancies in comparison with data recorded using the pendant drop technique. The Wilhelmy plate was cleaned with water and ethanol and was then dried with a Bunsen burner immediately before each measurement. The plate was hung on the surface pressure balance and was then immersed in pure water to achieve a surface tension of  $\gamma = 71.8 \pm 0.5$  mN m<sup>-1</sup> to ensure the cleanliness of the dish and the good performance of the plate. Afterward, the plate was used to measure the surface tension of many P/S solutions with the same cleaning procedure as described above repeated between each measurement. In every case, the data are presented at a surface age of 30 min (data were averaged over the time scale 29.8–30.2 min).

The measurements presented in Figure 10 were recorded on a home-built pendant drop shape analysis apparatus where 250  $\mu$ L was removed from each 20 mL sample rather than the larger volumes required for the Wilhelmy plate method. The experimental setup has been described elsewhere.<sup>70</sup> The pendant drop was created at the tip of a PTFE capillary which joined a gastight Hamilton syringe placed in a computer-controlled syringe pump. The drops were formed in a closed, temperature-controlled chamber with an internal size of 1  $\times$  2  $\times$  5 cm. To avoid evaporation of the pendant drop, the side walls of the chamber were covered with wetted filter paper. The applied experimental procedure was as follows: by turning on the syringe pump, a series of drops were formed at the tip of the capillary, thus ensuring the creation of a clean surface. The time required for the formation of a pendant drop was approximately 1 s. After the formation of the third pendant drop, the syringe pump was stopped, and the monitoring of the drop shape started ( $t = 0$ ). A picture of the pendant drop was taken every  $\sim 2$  s, and then the recorded sequential digital images were used for the calculation of the temporary surface tension values giving rise to the surface tension versus time function.

**UV–vis Spectroscopy Measurements.** Pdadmac/SDS/NaCl solutions were also measured using a UV–vis spectrometer (Jasco V-630 spectrophotometer) using a quartz Helma cell with a 1 mm path length. The turbidity was then evaluated according to the optical density at wavelength 450 nm. A spectrum of each solution was measured within 30 min of its preparation for surface tension measurements.

**Neutron Reflectometry Measurements.** NR measurements were performed on the new horizontal neutron reflectometer FIGARO at Institut Laue-Langevin (Grenoble, France).<sup>71</sup> The time-of-flight instrument was used with a chopper pair giving neutron pulses with 5.6%  $d\lambda/\lambda$  in the wavelength range  $\lambda = 2$ –30 Å. Data acquisitions were carried out at fixed incident angles of  $\theta = 0.62^\circ$  and  $3.8^\circ$  for an average acquisition time of less than 1 h each. Reflectivity data were normalized relative to an air/D<sub>2</sub>O measurement. Samples were left to reach steady state for at least 2 h prior to each measurement, and the satisfactory matching of data from the two different incident angles showed that the interfacial layers were not changing significantly during the measurements. The neutron reflectivity profiles presented show the intensity ratio



of neutrons in the specular reflection to those in the incident beam with respect to the momentum transfer,  $Q$ , defined by

$$Q = \frac{4\pi \sin \theta}{\lambda} \quad (1)$$

Samples for each compositional measurement of the surface excesses of polymer and surfactant in Figures 3, 6, and 8 were made in three isotopic contrasts: Pdadmac–dSDS/ACMW (air contrast matched water), Pdadmac–dSDS/D<sub>2</sub>O, and Pdadmac–hSDS/D<sub>2</sub>O. We noted that precipitate floated in the latter contrast, whereas it sank for the other two contrasts and for Pdadmac–hSDS/H<sub>2</sub>O samples discussed elsewhere in this work. Furthermore, the 2D detector image of the reflected neutrons revealed that the Pdadmac–hSDS/D<sub>2</sub>O samples gave significant off-specular scattering in the precipitation region, which was not observed from samples of the other two contrasts or from typical samples of thin, monomolecular adsorption layers. As the surfactant and solvent purities were both verified independently, we inferred that the Pdadmac–hSDS/D<sub>2</sub>O interfacial layers were not chemically equivalent to those of Pdadmac–dSDS/ACMW, Pdadmac–dSDS/D<sub>2</sub>O, and Pdadmac–hSDS/H<sub>2</sub>O due to density effects; i.e., the creaming of bulk aggregates occurred in that isotopic contrast only. Therefore, the Pdadmac–hSDS/D<sub>2</sub>O data were not considered in the data evaluation.

**Neutron Reflectometry Data Evaluation.** The criteria for selecting the appropriate layer model for fitting are that it is physically reasonable and has as few free fitting parameters as possible. We explored several options.

First, we applied a one adsorbed layer model, air–polymer/surfactant–subphase (as in the original NR work on this system<sup>41</sup>), which had the following implications. (1) The polyelectrolyte and surfactant form a uniform mixed adsorption layer. (2) The two isotopic contrasts are fitted independently. (3) The contrast Pdadmac–dSDS/ACMW gives the amount of surfactant (i.e., the scattering length density (SLD) of Pdadmac is approximated to zero). (4) The contrast Pdadmac–dSDS/D<sub>2</sub>O gives the amount of polymer (i.e., the SLD of dSDS is approximated to that of D<sub>2</sub>O). Two noteworthy limitations of this approach are as follows. First, the polymer itself has no significant hydrophobic moieties and does not adsorb at a bare air/water interface, and therefore it is evidently present at the interface as a result of interaction with the oppositely charged surfactant. In this respect, it follows that the polymer is electrostatically bound to the headgroups of a surfactant monolayer, and hence it effectively forms a spatially separated layer, with a different SLD, below the surfactant monolayer. Second, there are two values of a single interfacial layer SLD in any air–polymer/surfactant–D<sub>2</sub>O measurement that give equivalent fits, and given that there is a possibility of polymer loops beneath the monolayer and hence no packing limit that would constrain the layer SLD to one solution rather than the other, the choice of which fit to use would be arbitrary.

Next we considered a two adsorbed layer model, air–surfactant–polymer–subphase, which allowed us to quantify uniquely the amounts of polymer and surfactant at the interface and has the following implications. (1) The P/S complexes and free surfactant are positioned such that the alkyl chains of the surfactant are oriented toward the air, due to the hydrophobic driving force for adsorption, and the polyelectrolyte is positioned below the surfactant monolayer, due to the electrostatic attractive interaction and the hydrophilic character of the polymer. (2) The

two isotopic contrasts are comodeled to give consistent fits providing the surface excesses of polymer and surfactant. (3) The value of the SLD of the upper (surfactant) layer is effectively set by the magnitude of the reflectivity in the Pdadmac–dSDS/ACMW contrast, and the value of the SLD of the lower (polymer and solvent) layer is effectively set by the magnitude of the depletion in the SLD profile beneath the surfactant monolayer in the Pdadmac–dSDS/D<sub>2</sub>O contrast. (4) The polymer is assumed to be present only in the lower layer, which follows given that there is no driving force for adsorption at the air/water interface. (5) The residual surfactant in the lower layer is neglected for two reasons: (i) we know from the range of fitted layer thicknesses in the Pdadmac–dSDS/ACMW contrasts that there cannot be an appreciable quantity of surfactant aggregates, which would be on the scale of a few nanometers,<sup>72</sup> bound to the lower side of the polyelectrolyte, and (ii) electrostatic association of dodecyl sulfate ions in comparison with chloride ions must be low due to the fact that the surfactant concentration is 25–1000 times lower than that of the added inert electrolyte.

The third and most complicated model assumes a three adsorbed layer model. Here we considered two variants: air–surfactant/compact polymer/diffuse polymer–subphase and air–surfactant chains/surfactant headgroups with compact polymer/diffuse polymer–subphase. However, these approaches either required additional prior assumptions (e.g., neutrality of the surfactant headgroups in the latter case) or introduced at least one additional free fitting parameter.

We chose the two adsorbed layer model as giving unique, physically reasonable results while minimizing the number of free fitting parameters required. The fitting procedure involved iterating the thickness of the upper (surfactant) layer in the Pdadmac–dSDS/ACMW contrast followed by the thickness and volume fraction of the lower (polymer/solvent) layer in the Pdadmac–dSDS/D<sub>2</sub>O contrast to give a common model that satisfied both data sets from which the surface excesses of polymer and surfactant were calculated. The surfactant and polymer surface excesses,  $\Gamma_s$  and  $\Gamma_p$ , respectively, were calculated using

$$\Gamma_s = \frac{\sigma_s \cdot d_1}{b_s \cdot N_A} \quad (2)$$

and

$$\Gamma_p = \frac{\sigma_p \cdot d_2 \cdot v_{f,2}}{b_p \cdot N_A} \quad (3)$$

where  $\sigma_s$  and  $\sigma_p$  are the scattering length densities of the surfactant or polymer, respectively;  $d$  is the fitted layer thickness;  $v_f$  is the fitted volume fraction;  $b_s$  and  $b_p$  are the scattering lengths of the surfactant or polymer, respectively;  $N_A$  is Avogadro's number; the subscript 1 denotes a fitted parameter for the upper surfactant layer; and the subscript 2 denotes a fitted parameter for the lower polymer/solvent layer. The software Motofit was used,<sup>73</sup> which is based on the Abeles matrix model to calculate the reflectivity of thin layers and enables least-squares fitting of data from different isotopic contrasts.<sup>74</sup> An example of a typical set of reflectivity profiles with model fits is shown (Figure 1). Additional details about the fitting procedures and further examples of reflectivity profiles for different bulk compositions and physical sample states may be found in part 1 of the Supporting Information.

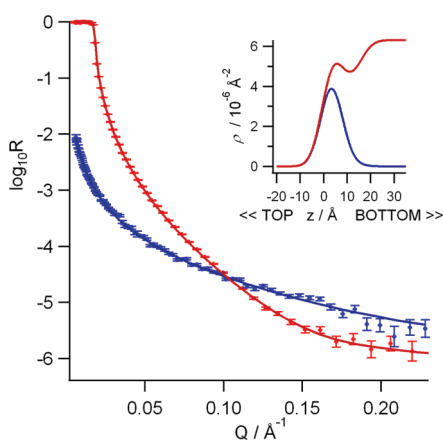


**Figure 1.** Example of neutron reflectivity profiles and model fits to the data of Pdadmac/SDS solutions recorded on FIGARO in less than one hour each: Pdadmac-dSDS/ACMW (blue) and Pdadmac-dSDS/D<sub>2</sub>O (red), where the bulk surfactant concentration was 0.62 mM and the samples were in the *aged-settled* state.

Note that the surfactant surface excess was determined by fitting the thickness of the surfactant layer with a volume fraction equal to unity (hence  $v_{f,1}$  is not a term included in equation 2). This model seems more physically realistic than fitting the volume fraction at fixed thickness given the substantial surfactant surface excesses determined for all the samples in this work. Also, the thickness and volume fraction of the polymer layer are correlated such that reliable comparisons of the polymer layer thickness from measurement to measurement were not possible. The data from all the solutions measured indicate a highly compact polymer film with a layer thickness of  $6.8 \pm 2.2$  Å and a volume fraction of  $63 \pm 17\%$ . Such a highly compact arrangement is consistent with theoretical<sup>75</sup> and experimental<sup>76</sup> work at the solid/liquid interface, as described in a recent review,<sup>77</sup> which showed that charged polyelectrolytes can bind in a very flat conformation since it is only next to the surface that the segment–segment repulsion can be counteracted by the segment–surface attraction. Given that there were no statistically significant changes in the layer thickness or volume fraction with changing bulk composition or sample state and given that the aim of these measurements is to determine the interfacial composition across the precipitation region with respect to the bulk phase behavior, we will focus on the analysis of the compositional data in the Results and Discussion sections.

**Gravimetric Analysis.** Pdadmac/SDS/NaCl solutions (300 mL) were prepared in 500 mL glass bottles and were left to age and settle for 3 days. After this time, 209 mL of the supernatant was removed with a glass pipet and was transferred into a large glass dish with known mass. It was dried through heating by steam from a water bath and then was placed in a vacuum drier at 60 °C for a few hours. The dish was removed warm from the vacuum drier and was placed to cool to ambient temperature in a desiccator (above dry calcium chloride) for 15 min. The heating and drying procedure was repeated (usually for 3 or 4 cycles) until constant mass was reached. The mass of the dry residue (Figure 5A) is corrected for the amount of salt to show the proportion of polymer dissolved or suspended in the solution (Figure 5B). This calculation is based on the simple approximation that there is an average stoichiometry of polymer/surfactant in the precipitate of unity; i.e., all the chloride ions in the polymer are replaced by dodecyl sulfate ions.

## RESULTS

We will examine the relationship between the surface properties and bulk phase behavior of Pdadmac/SDS solutions for three well-defined physical states of the system. The first is *fresh-mixed*, for which polymer and surfactant solutions are mixed then transferred at once to the measurement vessel. In the precipitation region, there is a suspension of aggregates present on a time scale of days. The second is *aged-settled* where the sample is prepared as above and left to equilibrate for 3 days. This is the time scale required for the bulk to reach steady state after which there is sediment and a supernatant that is virtually transparent. The third is *aged-redispersed* for which the only difference from the second category is that the samples are inverted once before measurement. The redispersion process applies a light mechanical stress to the settled precipitate, which has a marked effect on the surface properties.

In Figures 2–9 we present data from solutions of 100 ppm Pdadmac in 0.1 M NaCl with varying amounts of SDS where the gray shaded areas mark the precipitation region. There are four critical bulk compositions (i.e., different bulk SDS concentrations) which lie close to each other and are worth highlighting before we present the results.<sup>68</sup> First, there is the point where kinetically trapped P/S aggregates are sufficiently charged to retain their colloidal stability for much longer than a few days (0.48 mM SDS). Second, there is the edge of the precipitation region at which point the cliff edge peak in the surface tension is formed for the supernatant of aged samples (0.55 mM SDS). Third, there is the point of charge equivalence or stoichiometric mixing, where the number of moles of Pdadmac charges in the system equals that of dodecyl sulfate ions (0.62 mM SDS). Fourth, there is the point of charge neutrality of the complexes in the precipitation region, as determined using electrophoretic mobility measurements (0.82 mM SDS); for convenience, a figure of the experimental mobility data is reproduced from our recent letter<sup>68</sup> in part 2 of the Supporting Information. The four bulk compositions in question are marked with arrows a–d, respectively, in Figure 2B.

**1. Fresh-Mixed Samples.** We start our examination of the relationship between the bulk phase behavior and interfacial properties of Pdadmac/SDS solutions with *fresh-mixed* samples which exhibit the highest degree of aggregate dispersion of the three sample states investigated. These solutions are turbid in the precipitation region as shown by the high optical density (scattering of light at 450 nm), which indicates that there is a dispersion of P/S aggregates immediately after mixing the polyelectrolyte and surfactant (Figure 2A). On either side of the precipitation region, the turbidity is lower as the bulk complexes are sufficiently charged for a higher proportion of them to remain in the liquid phase. The surface tension of these solutions is constant at  $\sim 35$  mN/m for all the samples measured (Figure 2B), although in the precipitation region there is a small bump in the surface tension which is centered on the point of charge neutrality of the bulk complexes where aggregation is expected to be fastest. Despite this nascent peak in the surface tension, these data suggest that there is enough surface-active material in solution to form a substantial adsorption layer at the air/water interface, thus lowering its free energy over the whole range of bulk compositions.

The physical nature of this adsorbed material and its relationship to the phase behavior of the bulk and measured surface tension values were examined by recording NR data for

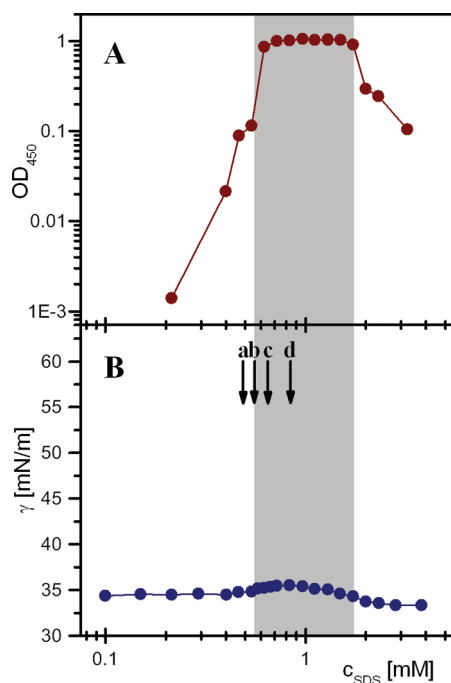


**Figure 2.** (A) Optical density at 450 nm recorded using UV–vis spectroscopy to indicate the turbidity and (B) surface tension at a surface age of 30 min of Pdadmac/SDS solutions, containing 100 ppm Pdadmac and 0.1 M NaCl, with respect to  $c_{\text{SDS}}$ , the bulk surfactant concentration. The data represent the *fresh–mixed* state. Lines are a guide to the eye only. The gray shaded area shows the precipitation region. Arrows a–d mark the four bulk compositions defined in the second paragraph of the Results section.

*fresh–mixed* solutions (Figure 3). As detailed in the Experimental Section, a two layer adsorption model, with a surfactant layer at the air/aqueous interface (formed due to hydrophobic interactions) situated above a layer of polyelectrolyte (electrostatically bound to the surfactant headgroups) fitted very well to the experimental data. At bulk SDS concentrations before the precipitation region, there are approximately the same number of moles of charged Pdadmac groups as SDS molecules at the interface in the samples measured, and the polymer layer is very compact with a thickness of  $<10$  Å (see Experimental Section for details), to which parallels may be drawn with the adsorption of charged polyelectrolytes on oppositely charged surfaces.<sup>77</sup> Hence these data suggest that the surface excess of polymer may be limited to that required for neutralization of the surfactant headgroups in the surface monolayer.

Up to about the point of charge neutralization of the complexes (0.82 mM), the surface excesses of polyelectrolyte and surfactant in the interfacial layer are remarkably constant with changing bulk composition. The simplest explanation is that the highly compacted polyelectrolyte layer effectively neutralizes the surfactant headgroup layer and is therefore in a state of steric saturation limited by the packing of the surfactant molecules in the surface monolayer. Across the precipitation region, the surface excess of polyelectrolyte decreases, which coincides with the transition in the bulk from positive to negative P/S complexes resulting in a reduction in their electrostatic attraction to the negatively charged surfactant headgroup layer. We attribute the resulting increase in surfactant surface excess to a decrease in penetration of polyelectrolyte molecules into the surfactant

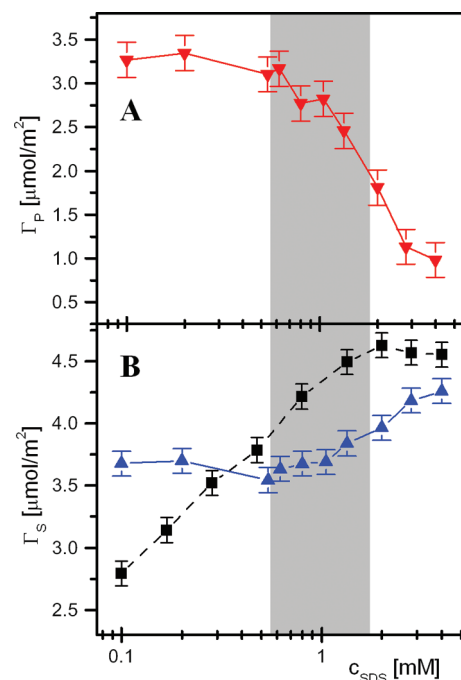


**Figure 3.** Surface excesses of (A) Pdadmac (red inverted triangles) and (B) SDS (blue triangles) in Pdadmac/SDS solutions and (B) pure SDS (black squares); data from pure SDS in 0.1 M NaCl are shown for reference. The P/S data represent the *fresh–mixed* state. Lines are a guide to the eye only. Data were recorded on the FIGARO reflectometer using NR. The gray shaded area shows the precipitation region.

headgroup layer, which reduces the steric barrier to the packing of surfactant molecules in the surface monolayer. It may be noted that at the highest surfactant concentrations measured there is still polymer at the interface, and the surfactant surface excess has not reached that of a full monolayer.

**2. Aged–Settled Samples.** To reveal the effects of bulk aggregation and precipitation on the interfacial behavior we measured the supernatant of *aged–settled* samples that had been left to equilibrate for 3 days. The solutions that were most turbid immediately after mixing became virtually transparent after 3 days due to the sedimentation of precipitate, as shown by the pronounced reduction in the optical density of these samples (Figure 4A). Precipitation occurs at bulk compositions close to charge neutrality of the complexes due to their lack of colloidal stability; i.e., the electrostatic repulsion between aggregates is not sufficient to stabilize the dispersion in the long term due to the low surface charge density of the P/S aggregates. On either side of the precipitation region, the samples remain turbid over much longer time scales than a few days. The particles present comprise kinetically trapped aggregates produced due to concentration gradients present during the first moments of mixing. The particles are therefore sufficiently charged to retain their colloidal stability for long periods. In these *aged–settled* samples there is a cliff edge peak in the surface tension with its maximum coinciding with the edge of the precipitation region (Figure 4B). The position of the maximum in the asymmetric peak occurs on the side of the precipitation region which has the lowest bulk surfactant concentration.

The pronounced sedimentation process made us question how much polymer and surfactant remained in the solution under the conditions where the cliff edge peak in the surface



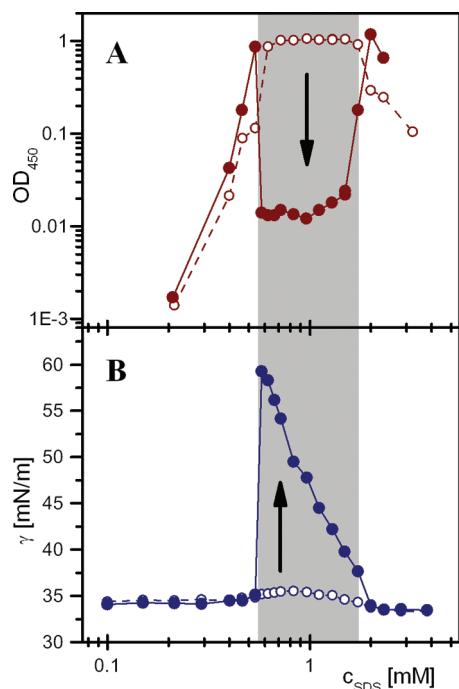


**Figure 4.** (A) Optical density at 450 nm recorded using UV–vis spectroscopy to indicate the turbidity and (B) surface tension at a surface age of 30 min of Pdadmac/SDS solutions. The data represent the *fresh–mixed* (open symbols) and *aged–settled* (closed symbols) states, and the arrows indicate the transitions between the two states. Lines are a guide to the eye only. The gray shaded area shows the precipitation region.

tension is produced. Gravimetric analysis was carried out on the supernatant of samples that were aged for 3 days to determine the amount of material dissolved as free polymer or individual P/S complexes or suspended as P/S aggregates (Figure 5A). The dashed line shows the mass of the material expected if there is no depletion resulting from sedimentation: the contributions to the value are 0.584% NaCl, 0.010% Pdadmac, and a variable contribution from SDS. There is clearly a sharp depression in the data at both edges of the precipitation region indicating loss of material, which led us to question further the extent of depletion of material. A calculation of the percentage of material left dissolved or suspended in solution, based on the simple approximation that the precipitate comprises a stoichiometric charge ratio of diallyldimethylammonium and dodecyl sulfate ions, is also shown (Figure 5B). These results suggest that after 3 days, when the aggregates that are suspended in solution upon mixing have precipitated and settled, there is essentially no polymer left in the liquid phase. It may be noted that these data are not compatible with the assumption of a two-phase air/liquid equilibrium in the thermodynamic model of Bell et al. which approximates all of the polymer to be present in the liquid phase even in the precipitation region.<sup>55</sup> These results prompted us to investigate the effect of comprehensive solution depletion on the interfacial properties.

The surface excesses of Pdadmac and SDS do not change as a result of the extended equilibration process, to within the errors of the measurements, for bulk compositions outside the precipitation region (Figures 6A and 6B, respectively). We infer that the adsorption layers reach steady state, or local equilibrium, in a matter of minutes and are unaffected by the prolonged storage of

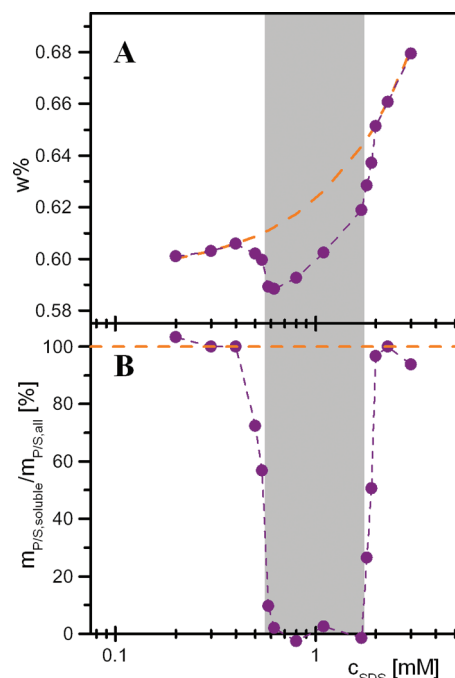


**Figure 5.** Gravimetric analysis of the supernatant of aged Pdadmac/SDS solutions: (A) percentage dry mass from solutions with 100 ppm Pdadmac and 0.1 M NaCl at different SDS concentrations and (B) the same data converted into the percentage of complexes dissolved or suspended in the solution phase (i.e., not precipitated and sunk) as detailed in the Experimental Section. In each case the dashed orange line shows the amount of material expected if all the surface-active material were to remain dissolved or suspended in the liquid phase after 3 days. The gray shaded area shows the precipitation region.

these samples. The situation in the precipitation region is quite different. We show clearly for the first time here that under the same experimental conditions—and at the same bulk composition—as the cliff edge peak in the surface tension, there are also sharp reductions in the surface excesses of polymer and surfactant. Polymer is evidently depleted from both the bulk solution and the interfacial layer only in the precipitation region, while the surfactant surface excess drops sharply at the edge of the precipitation region which has the least free surfactant and then gradually rises with increasing bulk surfactant concentration. There appears to be a crossover point in the surface excess of surfactant where it exceeds that from *fresh–mixed* solutions. This point, in keeping with our earlier interpretation that polymer bound electrostatically to the surfactant headgroups limits the packing of surfactant in the monolayer, indicates that a decrease in the amount of bound polymer results in an increase in the adsorbed amount of free surfactant due to packing constraints in the surface monolayer.

**3. Aged–Redispersed Samples.** To investigate the non-equilibrium nature of this system, we characterized a series of equivalent aged samples after the application of a light mechanical stress to the settled precipitate. The concept behind these measurements was to see if the redispersion of kinetically trapped aggregates could supply enough surface-active material to the air/water interface to result in a marked effect on the interfacial properties. The turbidity of *aged–redispersed* samples is affected minimally by the redispersion process, although the optical density decreases slightly. We attribute this observation to the effective filtration of residual small aggregates from the liquid

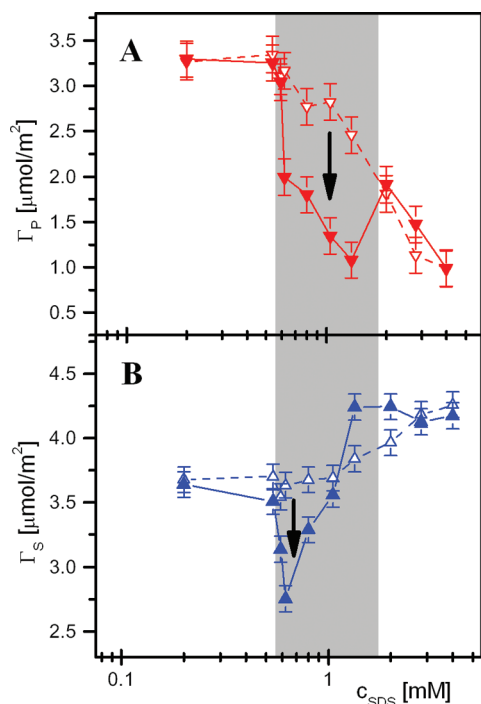


**Figure 6.** Surface excesses of (A) Pdadmac (red inverted triangles) and (B) SDS (blue triangles) in Pdadmac/SDS solutions. Data represent the *fresh*–*mixed* (open symbols) and *aged*–*settled* (closed symbols) states, and the arrows indicate the corresponding transitions. Lines are a guide to the eye only. Data were recorded on the FIGARO reflectometer using NR. The gray shaded area shows the precipitation region.

phase as they stick to large flocks that have been transported back into the bulk liquid by convection (Figure 7A). In contrast, there is a marked change in the surface tension as the cliff edge peak is now missing once again (Figure 7B). These results suggest that by simply inverting each sample in the precipitation region once we can release enough surface-active material into the liquid to result in a pronounced increase in the amount of adsorbed material at the air/water interface, and hence we have shown that the amount of interfacial material can be controlled by the choice of sample handling method applied.

The surface excesses of Pdadmac and SDS for these samples show that the amount and composition of material at the interface has effectively returned to values equivalent to those produced for samples measured moments after mixing (Figures 8A and 8B, respectively). There is no longer any sign of interfacial depletion, indicating that the mild redispersion process released enough material back into the liquid phase to form a substantial adsorption layer. Indeed, from the point-of-view of the surface excess and composition of interfacial material, simply by inverting each sample it appears that in a matter of seconds our actions reversed the effects of 3 days of bulk equilibration, although it must be pointed out that there are likely to be changes in the layer structure that were not resolved with the present experimental approach.

For aged samples, therefore, it follows that a range of interfacial excesses may be created—from an adsorption layer depleted of surface-active components with a high surface tension to packed layer with a low surface tension—simply by the way aged samples are handled. This demonstration outlines very clearly the inherent nonequilibrium nature of the Pdadmac/SDS system.

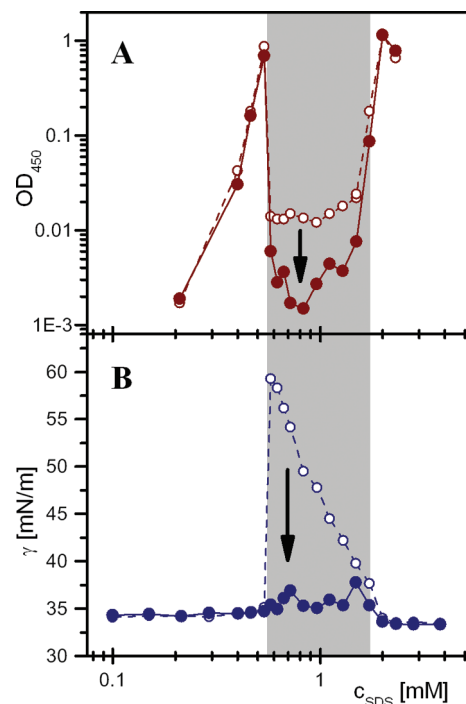


**Figure 7.** (A) Optical density at 450 nm recorded using UV–vis spectroscopy to indicate the turbidity and (B) surface tension at a surface age of 30 min of Pdadmac/SDS solutions. The data represent the *aged*–*settled* (open symbols) and *aged*–*redispersed* (closed symbols) states, and the arrows indicate the transitions between the two states. Lines are a guide to the eye only. The gray shaded area shows the precipitation region.

## DISCUSSION

**1. Does the Cliff Edge Peak in the Surface Tension Result Directly from Depletion of Surface-Active Material from the Air/Water Interface Due to Bulk Precipitation?** We start our discussion with an examination of the underlying reasons behind the cliff edge peak in the surface tension isotherm of the Pdadmac/SDS system. The equilibrium surface tension at a fluid interface in a multicomponent, two-phase system is described by the Gibbs's equation, which provides a differential relation between the surface tension ( $\gamma$ ) in the system and the surface excess ( $\Gamma$ ) of the components as a function of their chemical potential ( $\mu$ )<sup>78</sup>

$$d\gamma(\mu_2, \mu_3 \dots \mu_n) = - \sum_2^n \Gamma_i(\mu_2, \mu_3 \dots \mu_n) d\mu_i \quad (4)$$

where  $n$  is the number of components in the system and 1 denotes the solvent. The change of the surface tension between two equilibrium states of the system (A and B, respectively) can be given with the following integral equation<sup>3</sup>

$$\Delta\gamma(\mu_2, \mu_3 \dots \mu_n)_{A \rightarrow B} = - \sum_2^n \int_A^B \Gamma_i(\mu_2, \mu_3 \dots \mu_n) d\mu_i \quad (5)$$

Assuming that the system contains only surface-active ( $\Gamma > 0$ ) and nonsurface-active ( $\Gamma = 0$ ) components, as long as none of the chemical potentials of the components in the system decrease, the integral in equation 5 cannot be negative, and therefore the change in surface tension at constant temperature cannot be positive. In the investigated P/S system, measurements were performed at constant bulk polymer concentration as a function of increasing bulk



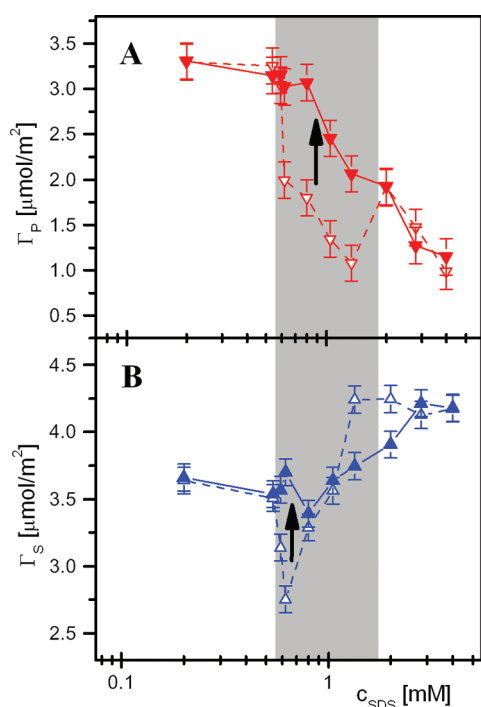


**Figure 8.** Surface excesses of (A) Pdadmac (red inverted triangles) and (B) SDS (blue triangles) in Pdadm/SDS solutions. Data represent the *aged-settled* (open symbols) and *aged-redispersed* (closed symbols) states, and the arrows indicate the corresponding transitions. Lines are a guide to the eye only. Data were recorded on the FIGARO reflectometer using NR. The gray shaded area shows the precipitation region.

surfactant concentration, which means that the surfactant chemical potential in the system never decreases. Thus, a sudden increase of the equilibrium surface tension can only be interpreted in terms of a sudden decrease of the chemical potential of a surface-active polymer/surfactant complex, as the polymer is not surface active in the absence of the surfactant. To fulfill this requirement Staples et al.<sup>41</sup> suggested and later Bell et al.<sup>55</sup> modeled the competition between two different bulk polymer/surfactant complexes, of which one is surface active and the other is not. They reasoned that the sudden increase of the surface tension occurs because the surface-active complex is transformed into the nonsurface-active complex that is stable in the bulk liquid, i.e., the chemical potential of the surface-active component in the bulk drops.

In the present work, we have shown that the increase in the surface tension, thus the drop of the chemical potential of surface-active species in the system, results only after essentially all of the polyelectrolyte and most of the surfactant have precipitated out of the liquid phase into solid particulate due to the lack of colloidal stability of P/S complexes close to charge neutrality. We have also shown that this depletion of surface-active material from the bulk liquid results in a sharp reduction in the adsorbed amounts of polyelectrolyte and surfactant at the air/water interface. What remains to be demonstrated is whether this observed interfacial depletion can quantitatively account for the peak in the surface tension or whether the features in the data are merely coincidental. We will therefore carry out a simple test to resolve this issue.

Given that under the physical conditions where the surface tension peak appears there has been precipitation of essentially all of the polyelectrolyte out of the bulk liquid (cf. Figure 5), we

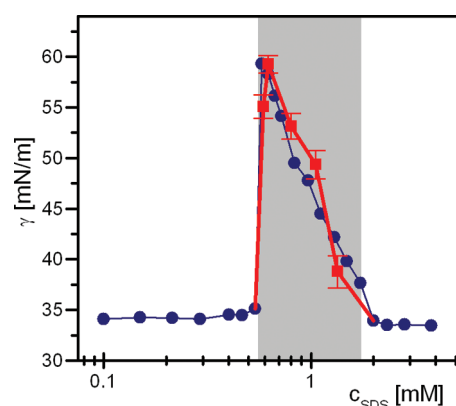


**Figure 9.** Surface tension at a surface age of 30 min of Pdadm/SDS solutions in the *aged-settled* (closed blue symbols) state and a calculation of the data from the corresponding surface excess of surfactant measured with NR in Figure 6B using the approximation that there is no polymer left in the liquid phase (red squares). Lines are a guide to the eye only. The gray shaded area shows the precipitation region.

may now test the approximation that there is in fact none left, thus reducing the system to three components: SDS, NaCl, and water. The two-phase equilibrium at the air/water interface may then be simplified—only in the precipitation region—to a depleted SDS monolayer, albeit perhaps also with embedded microparticles,<sup>45</sup> which if present in the form of solid-phase aggregates may explain the non-zero polymer surface excess shown in Figure 6A without there being a measurable effect on the surface tension. Hence with this approach we can take our measured surfactant surface excess values from Figure 6B and calculate corresponding surface tension values for the pure surfactant to see if there is also a pronounced cliff edge peak. This calculation was carried out with reference to a calibration plot between surface tension values from a previous study in the literature<sup>41</sup> and measure surface excess values from Figure 3B for pure SDS solutions in 0.1 M NaCl; see part 3 of the Supporting Information. The quantitative agreement between the calculated surface tension values from NR and the values measured directly is compelling (Figure 9) and helps us resolve two important issues.

First, concerning the bulk, our data are consistent with the comprehensive sedimentation of P/S complexes in the precipitation region. An implication is that data on bulk aggregation kinetics will form an important part of any model to predict the surface tension of an oppositely charged P/S mixture at a given time frame in the context of the evolving bulk phase behavior. Such data will also be required in studies of a range of systems to confirm whether steady state interfacial properties that may be reached in a matter of minutes or hours in fact represent steady state in the bulk or a system that is still slowly changing over a matter of days or longer.

Second, concerning the air/water interface, we have presented the first quantitative demonstration that the cliff edge peak in the surface tension can be explained by the lack of colloidal stability of P/S aggregates in the precipitation region, which over time leads to marked depletion of both polyelectrolyte and surfactant from the bulk liquid. The rise in surface tension is consistent with that expected from an adsorption layer of free surfactant at the air/water interface after comprehensive precipitation has taken place. This point is interesting in light of a recent suggestion that the surface

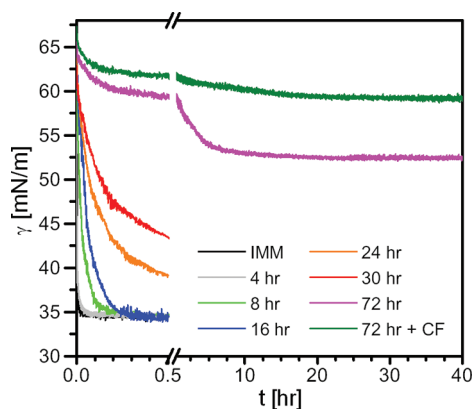


**Figure 10.** Kinetic surface tension data recorded as a function of time for the supernatant of Pdadmec/SDS solutions with 100 ppm Pdadmec, 0.62 mM SDS, and 0.1 M NaCl. The series of data represents the transition from *fresh*–*mixed* to *aged*–*settled* states, and the solution ages are stated in the legend. The uppermost trace (dark green line) represents a sample aged for 3 days then centrifuged (“CF” in the legend) to remove efficiently residual solid aggregates suspended in the liquid.

tension itself does not give an indication of what is taking place at the air/water interface.<sup>40</sup> An additional important implication of our work is related to the role of the nonsurface-active polymer/surfactant complex postulated by Staples et al.<sup>41</sup> and later used centrally in the equilibrium model by Bell et al.<sup>55</sup> to describe the present system. We have demonstrated that under the conditions of the high surface tension values in the precipitation region this species cannot be present significantly in the bulk liquid and that it is not required to rationalize the cliff edge peak in the experimental surface tension data.

**2. What is the “True Equilibrium” of the System in the Precipitation Region?** We have clearly demonstrated the inherent nonequilibrium nature of the Pdadmec/SDS system by producing either a depleted interface with a surface tension value of 60 mN/m or a packed interface with a surface tension of 35 mN/m for equivalent aged samples simply by changing the sample handling. Previous studies have discussed the “true equilibrium” of the system at the bulk composition corresponding to the top of the cliff edge peak in the surface tension and came up with different answers, which we will now consider in the context of our new experimental results.

Bell’s model states that the equilibrium surface tension is high.<sup>55</sup> They reasoned that the cliff edge peak in the surface tension results from the depletion of surface-active material from the interface due to a crossover in the favorability from bulk surface-active polymer/surfactant monomer complexes to non-surface-active polymer/surfactant micelle complexes. In contrast, Noskov et al. stated that the equilibrium surface tension is low.<sup>45</sup> They reasoned that the surface tension gradually decreased over many hours, and hence any measured high values are a transient state that has not yet reached equilibrium.

Like in the latter study, we will also follow the evolution of the system to predict true equilibrium, as thermodynamics states a system in a spontaneous process always approaches equilibrium. However, instead of looking at the surface tension kinetics for single samples, we follow the evolution of the surface tension as a function of the bulk equilibration time at a bulk surfactant concentration of 0.62 mM corresponding to the composition close to the top of the cliff edge peak (Figure 10). Here we used drop shape analysis for these measurements instead of a Wilhelmy

plate, so that much less solution could be extracted (250  $\mu$ L from 20 mL versus 50 mL from 100 mL), thus subjecting the settled precipitate to less mechanical stress and hence representing better the supernatant we were aiming to characterize.

We have already shown that the supernatants of samples at the left edge of the precipitation region which are equilibrated for 3 days have a high surface tension at a surface age of 30 min (i.e., the top of the cliff edge peak). When these samples are measured for much longer (up to 40 h), the surface tension drifts down slowly from 60 mN/m before reaching steady state at 53 mN/m after about 24 h. The initial reduction might be expected from the work of Noskov et al.,<sup>45</sup> but here it is not as dramatic, perhaps due to the specific measures we took to avoid redispersion to the settled precipitate. Further, if equivalent samples are centrifuged to remove the residual solid aggregates from the liquid phase, the surface tension maintains a value of  $\sim$ 60 mN/m for up to 40 h. These aggregates may exist in the samples because of the way the supernatant was extracted or perhaps because even after 3 days of equilibration the sedimentation process is not absolute. This higher steady state value implies that the slight reduction in the surface tension over many hours of the supernatant of aged samples is related to the presence of residual solid aggregates in the system, which supply the interface with surface-active material.

In summary, by following the effect on the surface tension of the evolution of the bulk phase behavior over 3 days, and by limiting the amount of redispersed aggregates present in the supernatant of aged samples, we have shown that the system evolves in the direction of high surface tension values which do reach steady state. Hence, like Bell et al.,<sup>55</sup> we conclude that the samples that exhibit the cliff edge peak are the closest of the three physical states studied to the “true equilibrium” of the system, but we do so for a very different reason. Our rationalization of the high surface tension values is that the high free energy at the air/water interface is compensated by low free energy of this multiphase system as a whole, including the solid precipitate and at the solid/liquid interface.

We propose that the “true equilibrium” state of the system in the precipitation region would involve the following: (1) a macroscopic air phase, (2) a liquid phase depleted of surface-active material due to the lack of colloidal stability of the Pdadmec/SDS complexes close to their charge neutrality, (3) a depleted air/water interface comprising free surfactant thus giving an asymmetric cliff edge peak in the surface tension, and (4) a solid phase comprising aggregates in the form of a single crystal. In actual samples, the aggregation process, which starts to happen on the first moments of mixing the components, continues for a few days until the precipitation process is comprehensive and the bulk has reached steady state. The sediment consists of kinetically trapped particles, which can be perturbed easily from their energy minima to refuel the liquid phase with bulk aggregates which consequently supply the air/water interface with surface-active material. The sample state that produces the cliff edge peak in the surface tension is indeed closest to the “true equilibrium”, but in practical terms the system has such a shallow minimum in free energy that it is hard to maintain. On practical time scales the “true equilibrium” of the system is inaccessible.

## SUMMARY AND OUTLOOK

We have outlined the reasons for the generation of a cliff edge peak in the surface tension isotherm of Pdadmec/SDS solutions. The high surface tension values in the peak region are caused by comprehensive precipitation of polyelectrolyte and most of the surfactant into solid particulate, which over a few days settles

under gravity to leave a bulk liquid that is virtually transparent and is highly depleted of surface-active material. Measurements of the surface composition of these samples reveal a sharp drop in the surface excesses of both polymer and surfactant at the bulk composition where the peak occurs, which is at the edge of the precipitation region, close to but not coinciding with the points of charge equivalence or charge neutralization of the complexes. The agreement between the measured surface tension values and a peak generated by calculation from the surface excess of surfactant in the precipitation region, using the approximation that there is no polymer left in the liquid phase, is remarkable. Across the precipitation region, the residual free surfactant in the bulk solution adsorbs at the air/water interface to form a depleted monolayer. The bulk composition at which the asymmetric peak in the surface tension occurs coincides with both the lowest bulk surfactant concentration and the lowest surfactant surface excess in the precipitation region, which rationalizes the striking asymmetric shape of the cliff edge peak.

The work involved a series of NR, surface tension, and UV–vis spectroscopy measurements recorded as a function of three well-defined physical states of the system. All of these samples involved static air/liquid interfaces whose physical properties had reached a reasonable steady state or local equilibrium, but none of the systems had in fact reached equilibrium, which cannot be accessed on practical time scales. Indeed we have demonstrated the production of two very different interfacial states from equivalent aged samples: the supernatant produces a depleted adsorption layer and a high surface tension because most of the surface-active material has precipitated out of solution, yet just a light mechanical stress applied to the precipitate results in redispersion of enough aggregates to supply the air/water interface with surface-active material forming a packed adsorption layer and a low surface tension. These results emphasize the inherent nonequilibrium nature of the system and question any assumptions concerning the applicability of chemical equilibrium to oppositely charged polymer/surfactant mixtures.

While the compelling image of data from the Pdadm/SDS system is the striking cliff edge peak in the surface tension, our findings imply that materials exhibiting such a condition are most likely to be found in a highly controlled laboratory setting. The precipitation process that causes the peak, however, is highly relevant to processes such as spraying that operate under dynamic conditions, as interfacial adsorption can be limited in the precipitation region by the slow diffusion of macroscopic aggregates. We have shown that steady state properties at the static air/water interface of an oppositely charge polyelectrolyte/surfactant mixture can be rationalized in terms of the nonequilibrium nature of the system with respect to the slowly changing bulk phase behavior. The implications for related systems are that while the surface excess and composition of material at the air/water interfaces may reach a reasonable steady state in a matter of minutes or hours the state of bulk aggregation could still be changing on a time scale of days or longer. Furthermore, in practical applications, even after the bulk has reached steady state, the physical properties of interfaces are likely to be dominated by material that has been perturbed from its energy minimum simply by the way the material is handled.

## ■ ASSOCIATED CONTENT

**S Supporting Information.** Further details about the NR data evaluation and additional reflectivity profiles, the point

of charge neutrality of the bulk complexes measured by electrophoretic mobility, and the calibration plot of surface tension to surface excess for SDS solutions in 0.1 M NaCl. This material is available free of charge via the Internet at <http://pubs.acs.org>.

## ■ AUTHOR INFORMATION

### Corresponding Author

\*E-mail: [campbell@ill.eu](mailto:campbell@ill.eu) and [imo@chem.elte.hu](mailto:imo@chem.elte.hu).

## ■ ACKNOWLEDGMENT

This work was supported within the 7th European Community RTD Framework Program by the Marie Curie fellowship PE-NANOSTRUCTURES by the Marie Curie European Reintegration Grant PE-NANOCOMPLEXES (PERG02-GA-2007-2249), the Hungarian Scientific Research Fund OTKA H-07A 74230, the Swedish Foundation for Strategic Research (RMA08-0056), and the Linnaeus grant “Organizing Molecular Matter” (OMM). I.V. is a Bolyai János fellow of the Hungarian Academy of Sciences which is gratefully acknowledged. We thank ILL for allocations of neutron reflectometry beam time on FIGARO and for the studentship support for A.A.S., and we thank Kriszta Sebestyen for assistance with the gravimetric measurements.

## ■ REFERENCES

- (1) Goddard, E. D. *Colloids Surf.* **1986**, *19*, 301–329.
- (2) Thalberg, K.; Lindman, B. Polymer–surfactant interactions – recent developments. In *Interactions of Surfactants with Polymers and Proteins*; Goddard, E. D., Ananthapadmanabhan, K. P., Eds.; CRC Press: Boca Raton, FL, 1993.
- (3) Kwak, J. C. T., Ed. *Polymer-Surfactant Systems*; Marcel Dekker: New York, 1998; Vol. 77.
- (4) Veis, A. *Biological Polyelectrolytes*, 1st ed.; Marcel Dekker, Inc.: New York, 1970; Vol. 3.
- (5) Malmsten, M. *Soft Matter* **2006**, *2*, 760–769.
- (6) Lapitsky, Y.; Zahir, T.; Shoichet, M. S. *Biomacromolecules* **2008**, *9*, 166–174.
- (7) Kogej, K.; Skerjanc, J. In *Surfactant Science Series*; Radeva, T., Ed.; Marcel Dekker Inc.: New York, 2001; Vol. 99, p 793.
- (8) Holmberg, K.; Jönsson, B.; Kronberg, B.; Lindman, B. *Surfactants and Polymers in Aqueous Solution*, 2nd ed.; John Wiley & Sons, Ltd.: New York, 2007.
- (9) Hansson, P.; Lindman, B. *Curr. Opin. Colloid Interface Sci.* **1996**, *1*, 604–613.
- (10) Bergfeldt, K.; Piculell, L.; Linse, P. *J. Phys. Chem.* **1996**, *100*, 3680–3687.
- (11) Hansson, P. *Langmuir* **2001**, *17*, 4167–4180.
- (12) Claesson, P. M.; Dedinaite, A.; Mészáros, R.; Varga, I. Association between Polyelectrolytes and Oppositely Charged Surfactants in Bulk and at Solid/Liquid Interfaces. In *Colloid Stability and Application in Pharmacy*; Tadros, T., Ed.; Wiley: New York, 2007; Vol. 3.
- (13) Allen, R. J.; Warren, P. B. *Langmuir* **2004**, *20*, 1997–2009.
- (14) Naderi, A.; Claesson, P. M.; Bergstrom, M.; Dedinaite, A. *Colloid Surf. A* **2005**, *253*, 83–93.
- (15) Naderi, A.; Claesson, P. M. *J. Dispersion Sci. Tech.* **2005**, *26*, 329–340.
- (16) Mezei, A.; Mészáros, R.; Varga, I.; Gilányi, T. *Langmuir* **2007**, *23*, 4237–4247.
- (17) Mészáros, R.; Thompson, L.; Bos, M.; Varga, I.; Gilányi, T. *Langmuir* **2003**, *19*, 609–615.



- (18) Mezei, A.; Pojjack, K.; Mészáros, R. *J. Phys. Chem. B* **2008**, *112*, 9693–9699.
- (19) Mezei, A.; Mészáros, R. *Soft Matter* **2008**, *4*, 586–592.
- (20) Nylander, T.; Samoshina, Y.; Lindman, B. *Adv. Colloid Interface Sci.* **2006**, *123–126*, 105–123.
- (21) Dahlgren, M. A. G.; Walthermo, A.; Blomberg, E.; Claesson, P. M.; Sjöström, L.; Åkesson, T.; Jonsson, B. *J. Phys. Chem.* **1993**, *97*, 11769–11775.
- (22) Dahlgren, M. A. G.; Hollenberg, H. C. M.; Claesson, P. M. *Langmuir* **1995**, *11*, 4480–4485.
- (23) Sukhishvili, S. A.; Dhinojwala, A.; Granick, S. *Langmuir* **1999**, *15*, 8474–8482.
- (24) Mészáros, R.; Varga, I.; Gilanyi, T. *Langmuir* **2004**, *20*, 5026–5029.
- (25) Varga, I.; Mezei, A.; Mészáros, R.; Claesson, P. M. *Soft Matter* **2011**, *7*, 10701–10712.
- (26) Pagac, E. S.; Prieve, D. C.; Tilton, R. D. *Langmuir* **1998**, *14*, 2333–2342.
- (27) Braem, A. D.; Prieve, D. C.; Tilton, R. D. *Langmuir* **2001**, *17*, 883–890.
- (28) Berglund, K. D.; Przybycien, T. M.; Tilton, R. D. *Langmuir* **2003**, *19*, 2705–2713.
- (29) Rojas, O. J.; Claesson, P. M.; Berglund, K. D.; Tilton, R. D. *Langmuir* **2004**, *20*, 3221–3230.
- (30) Mészáros, R.; Thompson, L.; Varga, I.; Gilanyi, T. *Langmuir* **2003**, *19*, 9977–9980.
- (31) Dedinaite, A.; Claesson, P. M.; Bergström, M. *Langmuir* **2000**, *16*, 5257–5266.
- (32) Naderi, A.; Claesson, P. M. *Langmuir* **2006**, *22*, 7639–7645.
- (33) Lucassen, J.; Hollway, F.; Buckingham, J. H. *J. Colloid Interface Sci.* **1978**, *67*, 432–440.
- (34) Asnacios, A.; Langevin, D.; Argillier, J. F. *Macromolecules* **1996**, *29*, 7412–7417.
- (35) Asnacios, A.; Langevin, D.; Argillier, J. F. *Eur. Phys. J. B* **1998**, *5*, 905–911.
- (36) Bergeron, V.; Langevin, D.; Asnacios, A. *Langmuir* **1996**, *12*, 1550–1556.
- (37) Monteux, C.; Williams, C. E.; Meunier, J.; Anthony, O.; Bergeron, V. *Langmuir* **2004**, *20*, 57–63.
- (38) Monteux, C.; Llauro, M. F.; Baigl, D.; Williams, C. E.; Anthony, O.; Bergeron, V. *Langmuir* **2004**, *20*, 5358–5366.
- (39) Lu, J. R.; Thomas, R. K.; Penfold, J. *Adv. Colloid Interface* **2000**, *84*, 143–304.
- (40) Taylor, D. J. F.; Thomas, R. K.; Penfold, J. *Adv. Colloid Interface* **2007**, *132*, 69–110.
- (41) Staples, E.; Tucker, I.; Penfold, J.; Warren, N.; Thomas, R. K. *Langmuir* **2002**, *18*, 5147–5153.
- (42) Taylor, D. J. F.; Thomas, R. K.; Penfold, J. *Langmuir* **2002**, *18*, 4748–4757.
- (43) Vongsetskul, T.; Taylor, D. J. F.; Zhang, J.; Li, X.; Thomas, R. K.; Penfold, J. *Langmuir* **2009**, *25*, 4027–4035.
- (44) Penfold, J.; Tucker, I.; Thomas, R. K.; Zhang, J. *Langmuir* **2005**, *21*, 10061–10073.
- (45) Noskov, B. A.; Grigoriev, D. O.; Lin, S.-Y.; Loglio, G.; Miller, R. *Langmuir* **2007**, *23*, 9641–9651.
- (46) Noskov, B. A.; Loglio, G.; Miller, R. *J. Phys. Chem. B* **2004**, *108*, 18615–18622.
- (47) Noskov, B. A.; Loglio, G.; Miller, R. *Adv. Colloid Interface Sci.* **2011**, *168*, 179–197.
- (48) Lourette, M.; Tilton, R. D. *Colloid Surf. B* **2001**, *20*, 281–293.
- (49) Tonigold, K.; Varga, I.; Nylander, T.; Campbell, R. A. *Langmuir* **2009**, *25*, 4036–4046.
- (50) Dautzenberg, H.; Gornitz, E.; Jaeger, W. *Macromol. Chem. Phys.* **1998**, *199*, 1561–1571.
- (51) Nizri, G.; Lagerge, S.; Kamysny, A.; Major, D. T.; Magdassi, S. *J. Colloid Interface Sci.* **2008**, *320*, 74–81.
- (52) Nizri, G.; Magdassi, S.; Schmidt, J.; Cohen, Y.; Talmon, Y. *Langmuir* **2004**, *20*, 4380–4385.
- (53) Ábrahám, A.; Mezei, A.; Mészáros, R. *Soft Matter* **2009**, *5*, 3718–3726.
- (54) Taylor, D. J. F.; Thomas, R. K.; Hines, J. D.; Humphreys, K.; Penfold, J. *Langmuir* **2002**, *18*, 9783–9791.
- (55) Bell, C. G.; Breward, C. J. W.; Howell, P. D.; Penfold, J.; Thomas, R. K. *Langmuir* **2007**, *23*, 6042–6052.
- (56) Bell, C. G.; Breward, C. J. W.; Howell, P. D.; Penfold, J.; Thomas, R. K. *Colloid Interface Sci.* **2010**, *350*, 486–493.
- (57) Penfold, J.; Tucker, I.; Thomas, R. K.; Taylor, D. J. F.; Zhang, L.; Bell, C.; Breward, S.; Howell, P. *Langmuir* **2007**, *23*, 3128–3136.
- (58) Campbell, R. A.; Ash, P. A.; Bain, C. D. *Langmuir* **2007**, *23*, 3242–3253.
- (59) Staples, E.; Tucker, I.; Penfold, J.; Warren, N.; Thomas, R. K. *Langmuir* **2002**, *18*, 5139–5146.
- (60) Deo, P.; Somasundaran, P. *Langmuir* **2005**, *21*, 3950–3956.
- (61) Varga, I.; Keszthelyi, T.; Mészáros, R.; Hakkel, O.; Gilanyi, T. *J. Phys. Chem. B* **2005**, *109*, 872–878.
- (62) Moglianetti, M.; Li, P.; Malet, F. L. G.; Armes, S. P.; Thomas, R. K.; Titmuss, S. *Langmuir* **2008**, *24*, 12892–12898.
- (63) Kristen, N.; Simulescu, V.; Vüllings, A.; Laschewsky, A.; Miller, R.; von Klitzing, R. *J. Phys. Chem. B* **2009**, *113*, 7986–7990.
- (64) Bykova, A. G.; Lin, S.-Y.; Loglio, G.; Lyadinskaya, V. V.; Miller, R.; Noskov, B. A. *Colloid Surf. A* **2010**, *354*, 382–389.
- (65) Buckingham, J. J.; Lucassen, J.; Holloway, F. J. *Colloid Interface Sci.* **1978**, *67*, 423–431.
- (66) Green, R. J.; Su, T. J.; Joy, H.; Lu, J. R. *Langmuir* **2000**, *16*, 5797–5805.
- (67) Jain, N.; Trabelsi, S.; Guillot, S.; McLoughlin, D.; Langevin, D.; Letellier, P.; Turmine, M. *Langmuir* **2004**, *20*, 8496–8503.
- (68) Campbell, R. A.; Angus-Smyth, A.; Yanez Arteta, M.; Tonigold, K.; Nylander, T.; Varga, I. *J. Phys. Chem. Lett.* **2010**, *1*, 3021–3026.
- (69) Dognon, A.; Abribat, M. C. *R. Acad. Sci. (Paris)* **1939**, *208*, 1881–1882.
- (70) Varga, I.; Keszthelyi, T.; Mészáros, R.; Hakkel, O.; Gilanyi, T. *J. Phys. Chem. B* **2005**, *109*, 872–878.
- (71) Campbell, R. A.; Wacklin, H. P.; Sutton, I.; Cubitt, R.; Fragneto, G. *Eur. Phys. J. Plus* **2011**, *126*, 107.
- (72) Vass, S.; Pedersen, J. S.; Pleštil, J.; Laggner, P.; Rétfalvi, E.; Varga, I.; Gilányi, T. *Langmuir* **2008**, *24*, 408–407.
- (73) Nelson, A. J. *Appl. Crystallogr.* **2006**, *39*, 273–276.
- (74) Abeles, F. *Ann. Phys.* **1948**, *3*, 504–520.
- (75) Ullner, M.; Woodward, C. E. *Macromolecules* **2002**, *35*, 1437–1445.
- (76) Dedinaite, A.; Ernstsson, M. *J. Phys. Chem. B* **2003**, *107*, 8181–8188.
- (77) Claesson, P. M.; Poptosheva, E.; Blomberg, E.; Dedinaite, A. *Adv. Colloid Interface Sci.* **2005**, *114–115*, 173–187.
- (78) Hunter, R. J. *Foundations of Colloid Science*; Clarendon Press: Oxford, UK, 1995; Vol. II.